SCIENTIFIC REPORTS

OPEN

SUBJECT AREAS:
MECHANISM OF ACTION
EXPERIMENTAL MODELS OF DISEASE
NATURAL PRODUCTS
TRANSCRIPTOMICS

Received
12 April 2013

Accepted
10 December 2013

Published
15 January 2014

Correspondence and requests for materials should be addressed to T.T. (tanaka@doc.medic.mie-u.ac.jp)

* These authors contributed equally to this work.

Eriocitrin ameliorates diet-induced hepatic steatosis with activation of mitochondrial biogenesis

Masanori Hiramitsu[1,7]*, Yasuhito Shimada[1,2,3,4,5]*, Junya Kuroyanagi[1], Takashi Inoue[7], Takao Katagiri[7], Liqing Zang[6], Yuhei Nishimura[1,2,3,4,5], Norihiro Nishimura[6] & Toshio Tanaka[1,2,3,4,5]

[1]Department of Molecular and Cellular Pharmacology, Pharmacogenomics and Pharmacoinformatics, Mie University Graduate School of Medicine, Mie, Japan, [2]Mie University Medical Zebrafish Research Center, Mie, Japan, [3]Department of Systems Pharmacology, Mie University Graduate School of Medicine, Mie, Japan, [4]Department of Bioinformatics, Mie University Life Science Research Center, Mie, Japan, [5]Department of Omics Medicine, Mie University Industrial Technology Innovation Institute, Mie, Japan, [6]Department of Translational Medical Science, Mie University Graduate School of Medicine, Mie, Japan, [7]Central Laboratory, Pokka Sapporo Food & Beverage Ltd., Aichi, Japan.

Lemon (*Citrus limon*) contains various bioactive flavonoids, and prevents obesity and obesity-associated metabolic diseases. We focused on eriocitrin (eriodictyol 7-rutinoside), a powerful antioxidative flavonoid in lemon with lipid-lowering effects in a rat model of high-fat diet. To investigate the mechanism of action of eriocitrin, we conducted feeding experiments on zebrafish with diet-induced obesity. Oral administration of eriocitrin (32 mg/kg/day for 28 days) improved dyslipidaemia and decreased lipid droplets in the liver. DNA microarray analysis revealed that eriocitrin increased mRNA of mitochondrial biogenesis genes, such as mitochondria transcription factor, nuclear respiratory factor 1, cytochrome c oxidase subunit 4, and ATP synthase. In HepG2 cells, eriocitrin also induced the corresponding orthologues, and reduced lipid accumulation under conditions of lipid loading. Eriocitrin increased mitochondrial size and mtDNA content, which resulted in ATP production in HepG2 cells and zebrafish. In summary, dietary eriocitrin ameliorates diet-induced hepatic steatosis with activation of mitochondrial biogenesis.

Non-alcoholic fatty liver disease (NAFLD) is associated with the metabolic syndrome, especially obesity, hyperlipidaemia and diabetes[1], and is now the most common liver disease in both adults and children worldwide[2]. Regulation of lipid metabolism in the liver is critical to prevent the development of NAFLD, because NAFLD includes a spectrum ranging from simple steatosis to steatohepatitis (non-alcoholic steatohepatitis: NASH), which worsens to cirrhosis and sometimes hepatocellular carcinoma. The prevalence of NAFLD has been estimated as 17–33% in some countries[3], and ~10% of patients with NAFLD develop NASH and 8–26% of individuals with NASH progress to cirrhosis[4].

Recently, growing evidence from several epidemiological and clinical studies has indicated beneficial health effects of certain fruits and their components against obesity and its related diseases including dyslipidaemia. Citrus fruits, including lemon (*Citrus limon* Burm. f.), contain various polyphenols that have been shown to have several positive health effects, mainly involving glucose and lipid metabolism, in experimental animal models and humans[5–8]. Of all the bioactive molecules of lemon, eriocitrin (eriodictyol 7-rutinoside) is a major flavonoid[9] with antioxidant activity[10]. Eriocitrin has a suppressive effect on oxidative stress in diabetic rats[11] and a lipid-lowering effect in rats on high-fat and high-cholesterol diets[12]. However, the mechanism of regulation of hepatic lipid metabolism by eriocitrin has yet to be elucidated.

To investigate the lipid-lowering mechanism of eriocitrin, we administered oral eriocitrin to a zebrafish model of diet-induced obesity (DIO-zebrafish)[13]. Zebrafish is a small teleost that can be used for vertebrate models of human diseases[14–17]. The high degree of genetic conservation in zebrafish compared with mammals contributes to its emergence as a model for obtaining insights into fundamental human physiology[18]. In DIO-zebrafish, increases of body weight, plasma triglyceride (TG), and liver steatosis are highly consistent with obesity observed in humans and rodent models of DIO[13]. The histology of adipose tissue, such as the liver and visceral fat, is also similar[19], as is the pathophysiological pathway of visceral fat, to that in human adipose tissues[13]. In addition, we have demonstrated the anti-obesity mechanism of tomato[20] and green tea extract[21] using the DIO-zebrafish. Thus, DIO-zebrafish could be used to validate the mechanism of visceral adiposity and hepatic steatosis.

In this study, we conducted transcriptome analysis of eriocitrin feeding in DIO-zebrafish to investigate the mechanism of the lipid-lowering effect. We demonstrated that eriocitrin activated mitochondrial biogenesis *in vivo* and *in vitro*, which resulted in a protective effect against hepatic steatosis that was induced by DIO.

Results

Eriocitrin prevents diet-induced hyperlipidaemia and hepatic steatosis. We conducted eriocitrin feeding experiments to analyse their phenotypic effects on DIO-zebrafish for 4 weeks. The body weight of the overfeeding (OF) group was 1.6-fold higher ($P < 0.01$) than that of the normal feeding (NF) group at week 4 (Fig. 1a). The body length of the OF group was slightly longer than that of the NF group ($P < 0.05$, Fig. 1b). However, the body mass index (BMI), which was calculated by dividing the body weight (g) by the square of the body length (cm), was increased 1.4-fold in the OF compared with the NF zebrafish ($P < 0.01$; Fig. 1c). Plasma TG was also increased ($P < 0.05$) in the OF group (Fig. 1d). We fed eriocitrin-containing gluten granules to the DIO-zebrafish (32 mg/kg/day) for 4 weeks. Zebrafish ate all the eriocitrin-containing gluten granules within 5 min, and there was no appetite suppression during the feeding experiment (Supplementary Fig. S1). Eriocitrin administration did not result in a significant difference between the body weight and BMI (Fig. 1a and c), but eriocitrin significantly suppressed the increase in plasma TG in DIO-zebrafish ($P < 0.05$, Fig. 1d). However, the fasting blood glucose did not significantly differ between the eriocitrin-fed group and the others (Fig. 1e). Eriocitrin reduced lipid accumulation (red spots in Fig. 1f) in liver tissues more than overfeeding with vehicle gluten granules, which was consistent with the decrease in plasma TG.

Transcriptome analysis of the liver of eriocitrin-fed DIO-zebrafish. To reveal the therapeutic mechanism of eriocitrin against hepatic steatosis, we performed DNA microarray experiments on the liver tissues from eriocitrin-fed zebrafish. We compared the genome-wide expression profiles of zebrafish in the NF or OF groups with vehicle and eriocitrin (four groups in total) to identify genes related to improvement of hepatic steatosis. k-means/median clustering analysis defined 10 clusters, and revealed that clusters 7 and 10 were selectively altered in DIO-zebrafish fed with eriocitrin (OF + Erio group). The average expression levels of clusters 7 and 10 were significantly ($P < 0.001$) increased by eriocitrin feeding in the NF and OF groups. Expression levels were also significantly ($P < 0.001$) increased in the OF + Erio group compared with the NF + Erio group (Fig. 2a, 2b and Supplementary Fig. S2). These findings implied that these clusters were involved in the therapeutic mechanism of eriocitrin. In total, 282 probes of these clusters corresponded to 152 human orthologues (Supplementary Table S1). Analysis of the genes with altered expression by Gene Ontology (GO) category using GOstat[22] revealed that 20 of their 150 human orthologues (13.1%) were involved in ATP synthesis and mitochondrial electron transport (Table 1). The GO analysis was conducted in the category of biological process, and $P < 0.01$ was considered to be significant.

We conducted gene set enrichment analysis (GSEA) of DIO-zebrafish fed with gluten and eriocitrin. GSEA is a powerful method that can analyse expression of every functional group of genes[23], and it has been used to clarify the mechanisms of various clinical conditions and effects. GSEA showed that expression of 15 gene sets was significantly higher (false discovery rate < 0.2) in zebrafish fed with eriocitrin (Supplementary Table S2). GSEA revealed that the gene set "HUMAN_MITODB_6_2002" was significantly upregulated in DIO-zebrafish fed with an eriocitrin diet (Fig. 2c). HUMAN_MITODB_6_2002 is activated by peroxisome proliferator activated receptor γ coactivator 1 (PPARGC1)[24] and highly correlated with mitochondrial functions. GO analysis and GSEA suggested that eriocitrin ameliorated hepatic steatosis by activating mitochondrial functions and ATP synthesis.

To confirm the results of GSEA analysis, we conducted quantitative (q)RT-PCR analysis of genes related to lipid metabolism and mitochondrial biogenesis, including genes in DNA microarrays (Table 2). Eriocitrin feeding significantly upregulated the mRNA level of lipid metabolism genes, *pparab* (zebrafish homologue of human *PPARA*), *acox1* and *acadm* (Fig. 3a). In addition, *ppargc1al* (zebrafish homologue of human *PPARGC1A*, also called *PGC-1α*), a gene involved in fatty acid oxidation, showed a nonsignificant trend towards ($P = 0.36$) increased expression with eriocitrin feeding (Table 2). As for mitochondrial genes, an eriocitrin diet significantly upregulated the mRNA levels of *tfam* and *nrf1*, which are mitochondrial biogenesis markers, and *cox4i1* and *atp5j*, which are involved in ATP synthesis (Fig. 3c).

Eriocitrin induces gene expression related to mitochondrial function in HepG2 cells and reduced lipid accumulation. To examine whether the alterations in gene expression detected in eriocitrin-fed zebrafish could be extrapolated to human liver, we treated HepG2 human hepatocarcinoma cells with eriocitrin for 48 h. As for the genes involved in lipid metabolism, qRT-PCR showed that eriocitrin increased the mRNA levels of *ACADM* (Fig. 3b) in a dose-dependent manner. Unlike the results with zebrafish, *PPARA* and *ACOX1* were not affected by eriocitrin exposure. As for mitochondrial gene expression, eriocitrin increased *TFAM*, *COX4I1* and *ATP5J* expression in a dose-dependent manner (Fig. 3d), which was similar to the results observed for the zebrafish model (Fig. 3c).

To investigate the ability of eriocitrin to prevent lipid accumulation, the HepG2 cells were incubated in a medium containing palmitate to induce lipid-overloading conditions. Cultured HepG2 cells were treated with eriocitrin (30 μM) for 2 days and then exposed to 400 μM palmitate with or without eriocitrin. The total lipid levels were detected by Oil Red O staining. Co-treatment of HepG2 cells with palmitate and eriocitrin (Pal + Erio) significantly prevented cellular lipid accumulation ($P < 0.05$; Fig. 3e and f). qRT-PCR analysis of the same genes in lipid-loaded HepG2 cells (Supplementary Figs. S3 and S4) showed similar gene expression patterns to those that were observed from the DIO-zebrafish (Fig. 3a and c).

Eriocitrin activates mitochondrial biogenesis. From the results of the transcriptome analysis of eriocitrin treatment, we hypothesized that eriocitrin activates mitochondrial biogenesis. Thus, we performed mitochondrial staining using MitoTracker Red CMXRos, which stained the perinuclear region of the mitochondria. After 48 h incubation with 10 μM eriocitrin, the mitochondrial mass of HepG2 was significantly increased compared with that observed with vehicle treatment (Fig. 4a, b). The mitochondrial biogenesis process involves expression of nuclear-encoded proteins that are essential for replication of mtDNA. We measured mtDNA copy numbers by qRT-PCR. To assess mtDNA content per cell, we measured the number of copies of well-conserved single-copy genes. *PK* was used as a marker for nuclear DNA and *CYTB* for mtDNA, as described previously[25]. Treatment with eriocitrin for 72 h significantly increased the mtDNA content in a dose-dependent manner, which corresponded to results observed from the image analysis (Fig. 4c). Subsequently, activation of mitochondrial biogenesis resulted in an increase in intracellular ATP production by eriocitrin treatment (Fig. 4d).

To evaluate the effects of eriocitrin on whole animal physiology, we started eriocitrin exposure at 4 dpf zebrafish for 72 h. At 7 dpf, addition of 10 μM eriocitrin to the breeding water also increased the total ATP content of zebrafish (Fig. 4e), which was consistent with the results for HepG2 cells (Fig. 4d).

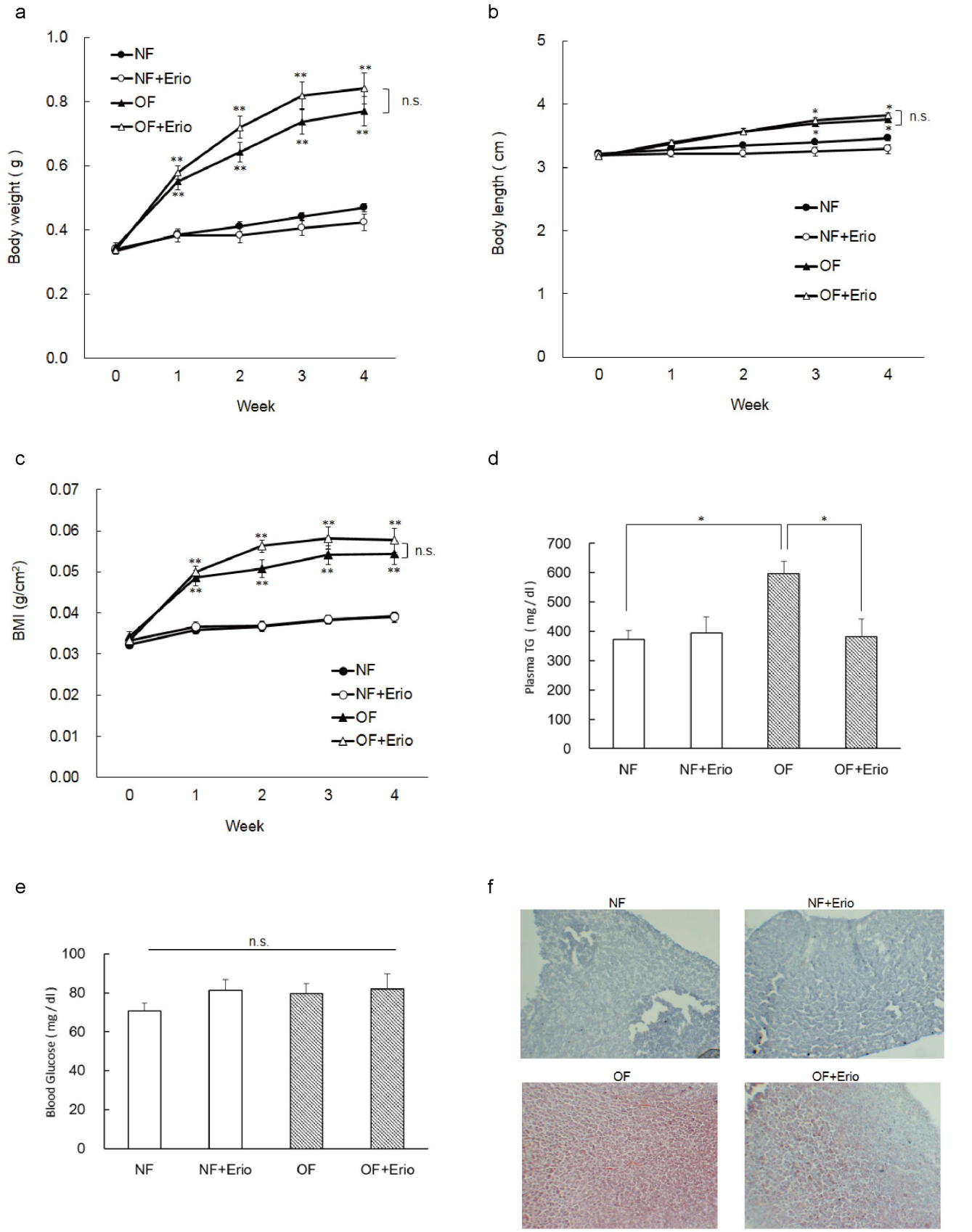

Figure 1 | Assessment of body weight and length, plasma TG, and hepatic steatosis in zebrafish overfed with eriocitrin. (a) Average body weight; (b) average body length; and (c) BMI in each group during 4 weeks feeding. Each group contained 10 fish. All values are mean ± SEM. $*P < 0.05$, $**P < 0.01$ versus vehicle in the NF group. (d) Plasma TG levels in each group. Four weeks' administration of eriocitrin reduced plasma TG in the OF group. Values are mean ± SEM; $n = 10$, $*P < 0.05$. (e) Fasting blood glucose in each group. Values are mean ± SEM; $n = 10$. (f) Oil Red O staining of liver sections. Eriocitrin reduced the number of lipid droplets (red) compared with the OF group. Erio: eriocitrin.

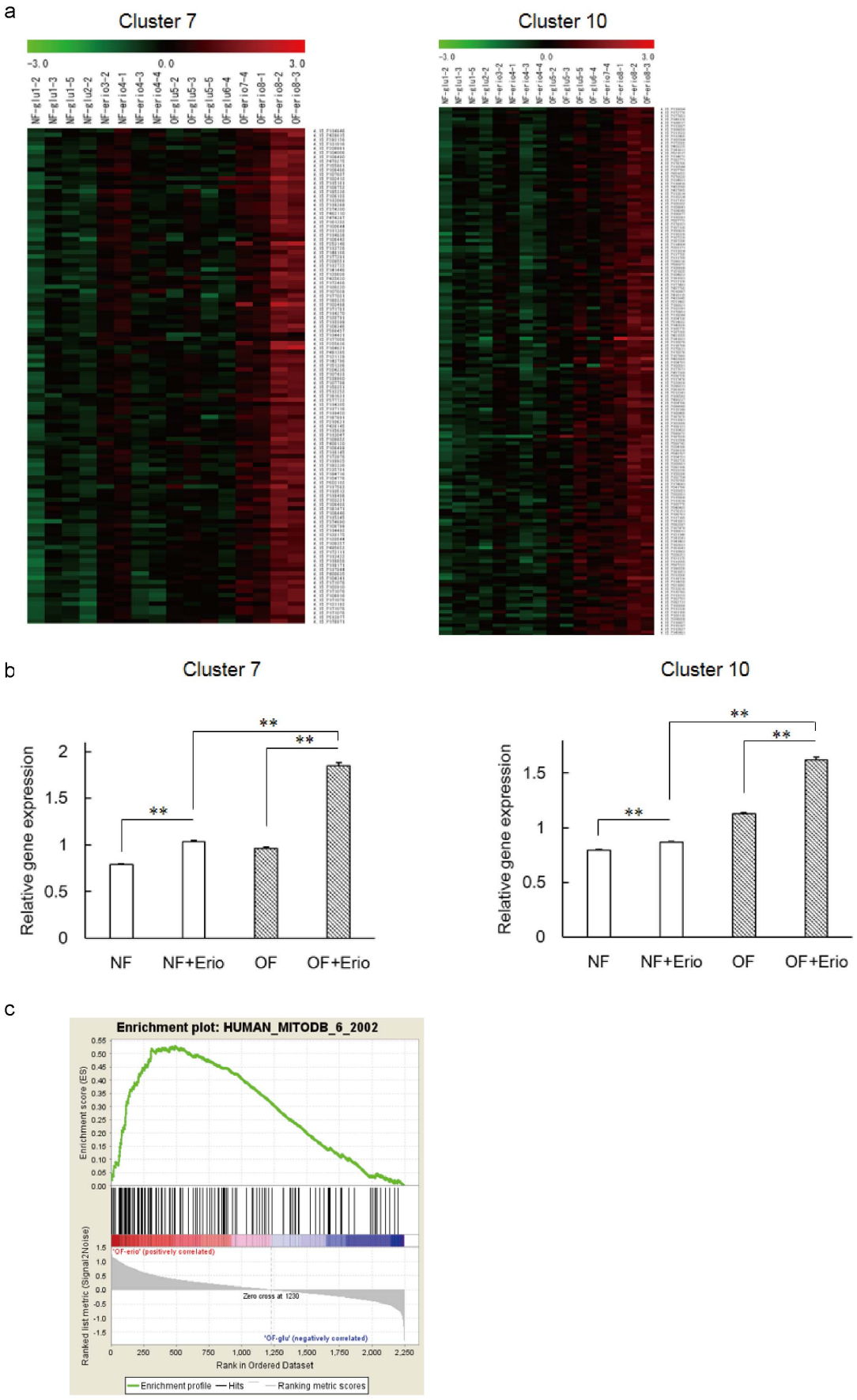

Figure 2 | Analysis of DNA microarray data. (a) Clustering analysis of DNA microarrays and (b) the average expression levels of clusters 7 and 10. (c) GSEA plots showed that expression of a mitochondrial gene module[24] was more enriched in the OF + Erio group compared with the OF group.

Table 1 | Ontology analysis of genes with altered expression (clusters 7 and 10 in Fig. 2a) in eriocitrin administration

Group	GO ID	GO Terms	genes	*P* value
ATP synthesis	GO:0006119	Oxidative phosphorylation	atp5o, ndufs3, atp5d, ndufa4, atp5h, ndufa8, atp5l, ndufa6, atp6v1f, hcg_25371, ndufb5, ndufs6, atp5c1, ndufb6, ndufb2, ndufb8, ndufa2	1.84E-17
	GO:0042775	Organelle ATP synthesis coupled electron transport	hcg_25371, ndufb5, ndufs6, ndufs3, ndufb6, ndufa4, ndufa8, ndufb2, ndufa6, ndufb8, ndufa2	1.30E-12
	GO:0009145	Purine nucleoside triphosphate biosynthetic process	atp5o, atp6v1f, atp5c1, atp5d, atp5j2, atp5h, nme1, atp5l	1.10E-06
	GO:0009108	Coenzyme biosynthetic process	atp5o, atp5h, atp6v1f, atp5l, atp5c1, atp5d, atp5j2	0.000211878
Electron transport	GO:0006120	Mitochondrial electron transport, NADH to ubiquinone	ndufb5, ndufs6, ndufs3, ndufb6, ndufa4, ndufa8, ndufb2, ndufa6, ndufb8, ndufa2	1.54E-12
	GO:0015985	Energy coupled proton transport, down electrochemical gradient	atp5o, atp5h, atp6v1f, atp5l, atp5c1, atp5d	1.39E-05
	GO:0015992	Proton transport	atp5o, atp5h, atp6v1f, atp5l, atp5c1, atp5d, atp5j2	2.07E-05
Other	GO:0006752	Group transfer coenzyme metabolic process	atp5o, atp5h, atp6v1f, atp5l, atp5c1, atp5d, atp5j2	2.39E-05
	GO:0006414	Translational elongation	rplp0, rplp1, eef1b2, rplp2	0.001341631
	GO:0051289	Protein homotetramerization	atpif1, pcbd1	0.006574703

Discussion

A lot of research has recently been conducted regarding the mechanism of the development of NAFLD, and a strong correlation has been observed between this mechanism and the origin of metabolic syndrome, mainly obesity. However, the genesis of obesity is multifactorial, and there is evidence that reduced energy expenditure, in particular reduced capacity to utilize fat for metabolic fuel, is an important factor, particularly in the weight-reduced state[26]. In obese people, therapeutics often target the mitochondria of metabolically active tissues such as skeletal muscle, liver, adipose tissues, and the heart[27]. There is also growing evidence that mitochondria have a key role in NAFLD[28,29]. Our studies demonstrated that eriocitrin suppressed the increase in serum TG and ameliorated hepatic steatosis through activation of mitochondrial biogenesis in DIO-zebrafish.

Eriocitrin is a stronger antioxidant than the other citrus flavonoid compounds and is abundant in lemon and lime[30], with safety proven by the lack of developmental toxicity in zebrafish (Supplementary Figs. S5 and S6). In addition, a rat feeding test revealed that lemon flavonoids containing 33% eriocitrin could be administered at ≤2 g/kg/day for 4 weeks without causing any toxicological phenotypic changes, including body weight, feeding volume, urine, haematological and biochemical parameters, organ weight, and histology (data not shown). There was no phenotypic change at ≤2 g/kg/day. This finding suggests that the lipid-lowering action of eriocitrin might be limited in lipid dysregulation (e.g., hyperlipidaemia). For example, naringin (a flavonoid found in citrus fruits) has been shown to also improve lipid profiles in a high-fat diet-induced model of obesity in rats, but there was no difference in the treatment group upon normal feeding[31]. Previous studies have focused on the lipid-lowering effects of eriocitrin on antioxidant defence mechanisms[10,11] but have provided little information on its effects on mitochondria. In our previous study using high-fat diet mice, crude extracts of the polyphenol fraction from lemon peel also ameliorated the symptoms of the metabolic syndrome, including dyslipidaemia, with expression of *Ppara* and *Acox1* (mitochondrial β-oxidation enzyme) in the liver[32]. Eriocitrin also increased *ppara* and other β-oxidation enzyme genes, *acox1* and *acadm*, suggesting that eriocitrin is the main antidyslipidaemic component in lemon polyphenols. Additionally, PPARA agonist ameliorated NAFLD in mice by modulating the genes for enzymes involved in fatty acid metabolism, including *Acox1* and *Acadm*[33], which was similar to eriocitrin-induced expression of *PPARA*.

Eriocitrin also increased the expression of genes involved in mitochondrial biogenesis (*NRF1* and *TFAM*) and ATP synthesis (*ATP5J* and *COX4I1*). NRF1 activates the transcription of several nuclear-encoded genes, especially mtDNA, and its liver-specific inactivation leads to hepatic steatosis and neoplasia[34], indicating that the therapeutic mechanism of eriocitrin is through *NRF1* induction. PPARGC1A regulates NRF1-dependent transcription[35] and increases expression of nuclear and mitochondrion-encoded genes of oxidative metabolism (lipid oxidation, and electron transport complexes) to promote mitochondrial biogenesis[36]. In addition, dietary restriction also increases mitochondrial respiration, with gene expression for PPARGC1A, NRF1 and cytochrome C oxidase subunit IV[37], which appears to be consistent with our results for eriocitrin. PPARGC1 also has a role in this pathway by activating NRF1 to induce expression of TFAM, which is important to the transcription of mtDNA[36,38]. Thus, in DIO-zebrafish and HepG2 cells, eriocitrin may also activate or induce PPARGC1, subsequently promote *NRF1* and *TFAM* expression to induce mitochondrial biogenesis and energy expenditure, and finally ameliorate hepatic steatosis. In spite of the eriocitrin-induced activation of mitochondria, we could not detect any antioxidant activity by DNA microarray analysis, except for upregulation of *prdx3*. Although oxidative phosphorylation is a vital part of the ATP production induced by eriocitrin, it also produces reactive oxygen species such as superoxide and hydrogen

Table 2 | qRT-PCR and DNA microarray results of eriocitrin administration

		qRT-PCR		DNA microarray	
Gene symbol	Gene ID	OF	OF + Erio	OF	OF + Erio
pparab	557714	0.37 ± 0.05	1.18 ± 0.28 *	nd	nd
acox1	449662	0.64 ± 0.12	1.24 ± 0.26	1.04 ± 0.21	1.02 ± 0.13
acadm	406283	0.73 ± 0.14	1.20 ± 0.14 *	0.98 ± 0.11	1.34 ± 0.13 *
cox4i1	326975	0.59 ± 0.05	1.21 ± 0.13 **	1.01 ± 0.03	1.43 ± 0.15 *
atp5j	406599	0.72 ± 0.06	1.03 ± 0.12 *	1.06 ± 0.10	1.72 ± 0.16 *
ppargc1a	553418	0.27 ± 0.18	0.46 ± 0.11	nd	nd
nrf1	64604	1.31 ± 0.32	3.43 ± 0.55 *	0.94 ± 0.16	1.04 ± 0.14
tfam	571106	0.42 ± 0.02	1.01 ± 0.12 *	0.78 ± 0.02	1.16 ± 0.10 *

All values are mean ± SEM; $n = 4$ or 5,
$^{*}P < 0.05$,
$^{**}P < 0.01$.

peroxide. This leads to propagation of free radicals, which damage cells and contribute to inflammatory disease, NASH and, possibly carcinogenesis. We hypothesized that eriocitrin-induced *prdx3* expression could prevent this pathway as an antioxidative mechanism. Oxidative stress coupled with hepatocyte apoptosis is believed to play a pivotal role in the pathogenesis of NAFLD[39,40]. In addition, emerging data now suggest that hepatocyte apoptosis may be a key component of the "second hit" involved in the progression of simple steatosis to NASH. In this context, several studies reported that antioxidants attenuate oxidative stress and hepatic steatosis; however, we could not detect the antioxidant properties of eriocitrin in the current study.

To predict the site of action of the therapeutic effects of eriocitrin, we conducted Sub-Network Enrichment Analysis (SNEA)[41] of our DNA microarray data. SNEA could identify key molecules regulating the expression of the genes involved in lipid metabolism and mitochondrial biogenesis. Although eriocitrin may influence multiple lipid-metabolizing pathways, similar to other polyphenols, we found

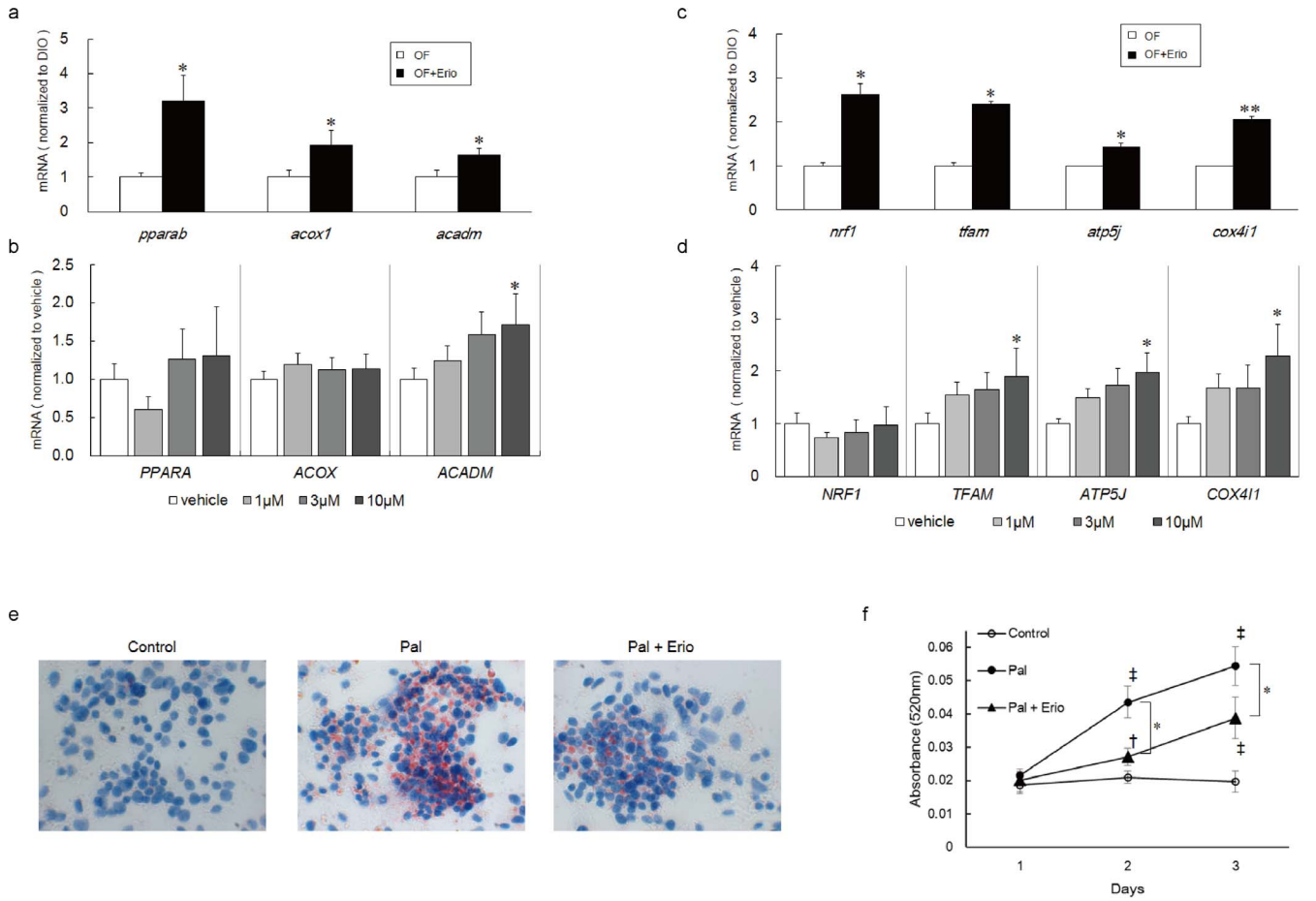

Figure 3 | qRT-PCR of genes related to lipid metabolism and mitochondrial functions, and eriocitrin reduced lipid accumulation in HepG2 cells. To confirm the DNA microarray analyses, qRT-PCR was conducted. Genes related to lipid metabolism in zebrafish (a) and HepG2 cells (b). Genes related to mitochondrial biogenesis and respiratory function in zebrafish (c) and HepG2 cells (d). All values are means ± SEM; $n = 5$, $^{*}P < 0.05$, $^{**}P < 0.01$. (e) Oil Red O staining of HepG2. (f) Absorbance of Oil Red O during lipid accumulation. Eriocitrin reduced lipid accumulation in palmitate-stimulated HepG2. All values are means ± SEM; $n = 8$, $^{*}P < 0.05$.

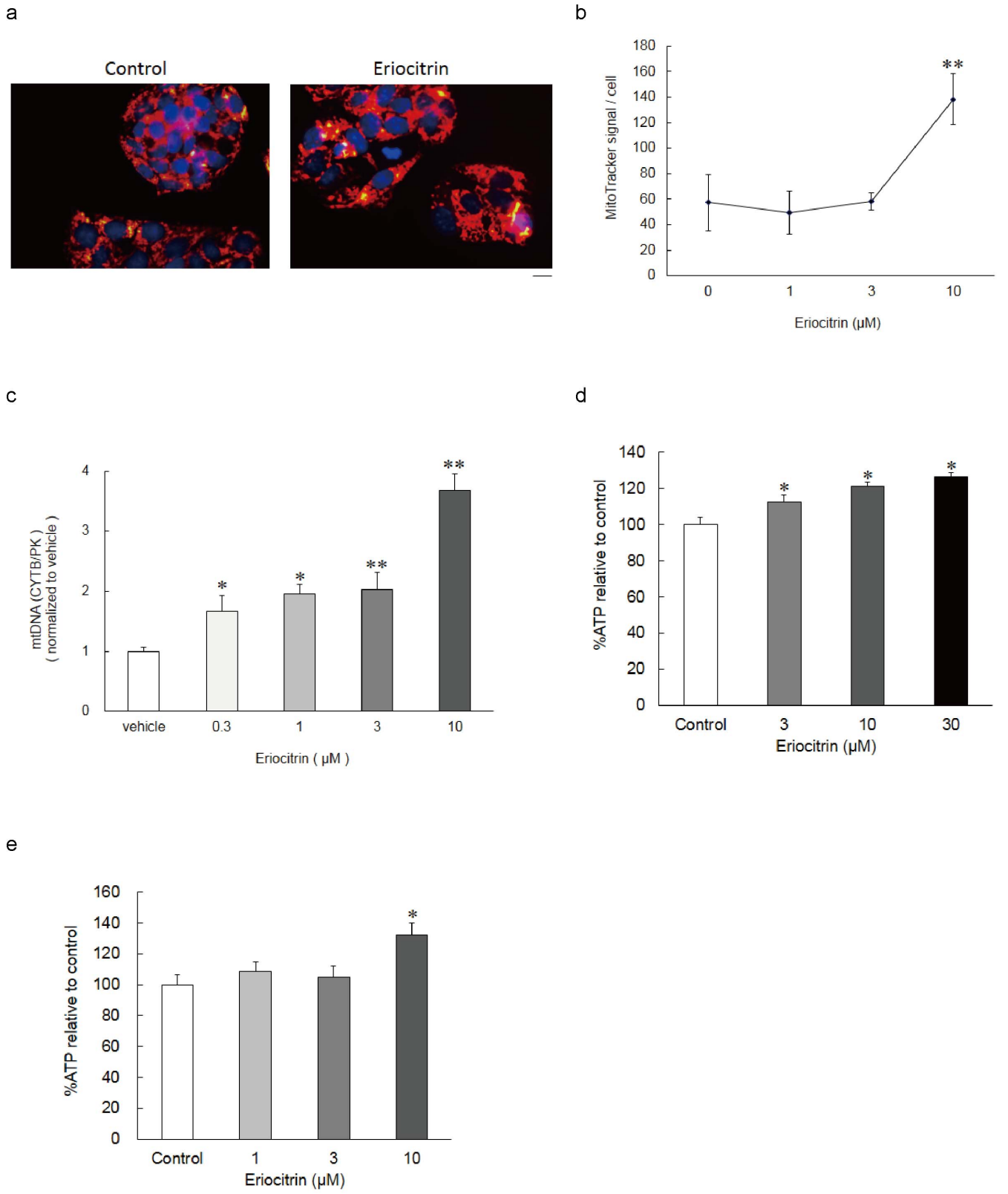

Figure 4 | Eriocitrin increased mitochondrial biogenesis and ATP production. (a) Eriocitrin (10 μM) increased mitochondrial size (red) of HepG2 cells using MitoTracker Red CMXRos staining. Blue colour represents the nucleus (Hoechst 33342). (b) Quantitative analysis of mitochondrial staining. (c) Quantification of mtDNA was accomplished by calculating the ratio of *CYTB* to nuclear *PK* and expressing it as mtDNA copy number per cell. (d), (e) ATP quantification with eriocitrin administration. Upon 72 h administration of eriocitrin, there were increased intracellular ATP in HepG2 cells (d) and systemic ATP of 7 dpf zebrafish (e). All values are mean ± SEM; $n = 8$, $^{*}P < 0.05$, $^{**}P < 0.01$.

Table 3 | Prediction of eriocitrin mechanism using SNEA

Gene set seed	Name	Total # of neighbours	# of measured neighbours	Measured neighbours	Median change	*P* value
RXR	Retinoid X receptor	248	68	APOA4, VEGFA, DDAH1, LCN2, FGFR1, CAV1, SCARB1, ABCC2, CYP27A1, FGB, HMOX1, MGP, ACOX1, CA2, NR1D1, ARG2, CYP8B1, VDR, ABCG5, LPL, CEBPA, PTPN6, RBP1, APOA1, CETP, DBI, FOS, MYOD1, ANGPTL3, THRB, BCL2, EGFR, BCL2L1, NDRG1, SLC2A2, ACADM, SLC27A2, ACLY, ACO1, PTH1R, CYP4A11, FABP1, GATA6, MEIS1, RXRG, COL1A2, PLIN2, SCP2, SLC27A1, CRABP1, CYBB, DUSP1, CCND1, ACACB, TRIB3, CYBA, ANGPTL4, ABCA1, NR1H4, NR1H3, HAND2, LDLR, SLC13A1, MAF, DCN, EGR1, RETN, SLC26A5	−1.017	0.004
SREBF1	Sterol regulatory element binding transcription factor 1	134	50	SLC2A2, CAV1, PTGDS, CEBPB, ABCA1, FABP1, CETP, ACSS2, HMGCS1, DBI, LPIN1, IRS2, PFKFB1, ACACB, ALDH1A2, INSIG1, VEGFA, PKLR, PDX1, SLC27A2, FDPS, HK2, RETN, ACLY, FADS2, ELOVL5, HMOX1, LPL, AR, HNF4A, LIPE, LIPC, CYP8B1, ACSL1, GNAI2, GPX3, PGD, CASP2, IDH1, HSD17B7, COL6A1, TRIB3, DHCR7, GPAM, SP1, HDC, LDLR, SCARB1, BAX, CEBPA	−1.055	0.005
STAT6	Signal transducer and activator of transcription 6	119	20	CAV1, BCL2, BAX, IGFBP1, COL1A2, BCL2L1, AICDA, AGT, IRS2, SOCS3, MUC5AC, IGF1, CDKN1B, MUC1, CLCA1, EGR1, MAF, PML, VCAM1, NFIL3	−1.450	0.006
CDX2	Caudal type homeobox 2	64	11	IRS2, HNF1A, CDH17, FABP2, HNF4A, VDR, ACAT2, SP1, HBEGF, LYPLA1, BCL2	1.328	0.007
MAPK11	Mitogen-activated protein kinase 11	36	11	SCARB1, BAX, BCL2, HMOX1, VDR, CEBPD, PRDX1, CAV1, CEBPB, EGR1, CCND1	1.025	0.007
Luteinizing hormone	-	69	15	LDLR, SCARB1, EGFR, AREG, CEBPD, RETN, C13orf15, KDR, IGFBP5, ANXA5, FLT1, IGFBP2, SGK1, PSEN1, CEBPB	−1.238	0.007
NKX2-5	NK2 homeobox 5	52	14	CALR, TLL1, CTNNB1, GATA4, PITX2, ACTC1, DIO2, MEF2A, ACACB, T, PLOD1, MYOD1, HOPX, ACTA2	−1.360	0.008
HEY1	Hairy/enhancer-of-split related with YRPW motif 1	23	11	MDM2, RUNX2, ID1, ACTA2, KDR, GATA4, GATA6, MYF5, OCLN, AR, PRODH2	−1.342	0.008
Runt	Runt-related transcription factor	50	9	BCL2, C13orf15, LGALS3, CEBPD, TGFBR1, BTG2, SP1, IL7R, RUNX2	−1.368	0.009

that two lipid metabolism pathways, retinoid X receptor (RXR) and sterol regulatory element-binding transcription factor 1 (SREBF1) pathways were significantly ($P < 0.01$) influenced by eriocitrin feeding (Table 3, underlined). Eriocitrin suppressed the RXR pathway, which was consistent with its antidyslipidaemic effects. PPARA regulates genes involved in lipid metabolism via heterodimerization with RXR as an obligate partner[42,43], suggesting interaction between eriocitrin and RXR, especially RXR-α. RXR antagonist HX531 has been reported to ameliorate obesity[44,45]; therefore, we hypothesize that eriocitrin acts as an RXR antagonist in liver adiposity. In fact, daidzein (a flavonoid found in soybeans) has been shown to suppress RXR-α expression[46] and improve lipid metabolism[47], which is in accordance with the prediction of RXR enrolment in eriocitrin pathways. Eriocitrin was also predicted to downregulate the SREBF1 pathway (Table 3). *Srebf1* is induced by heterodimerization of liver X receptor (LXR) and RXR[48], supporting the RXR hypothesis of eriocitrin described above. In addition, resveratrol, a polyphenol present in peanuts and grapes, has been reported to alleviate alcoholic fatty liver by inhibiting *Srebf1* expression via the Forkhead box o1 (Foxo1) signalling pathway[49]. *foxo1* was also decreased by eriocitrin in DNA microarray data, implying a similar mechanism for eriocitrin and resveratrol.

In conclusion, our observations using DIO-zebrafish and cultured human cells demonstrate a novel mechanism of powerful lipid-lowering activity of eriocitrin. Steatohepatitis is sometimes caused by hepatic steatosis and decreases the activity of respiratory chain complexes and impairs the ability to synthesize ATP in patients[50]. Eriocitrin promotes mitochondrial β-oxidation and biogenesis and ameliorates high-fat-diet-induced hepatic steatosis.

Methods

Ethical approval. This study has been approved by the Ethics Committee of Mie University, and was performed according to Japanese animal welfare regulation 'Act on Welfare and Management of Animals' (Ministry of Environment of Japan) and complied with international guidelines.

Preparation of eriocitrin. Eriocitrin was prepared from lemon peel using the modified method of Miyake *et al*[51]. The lemon peel was extracted using deionized water. The extract was applied to an Amberlite XAD-16 column (Rohm and Haas, Philadelphia, PA, USA). The column was washed with water, and eluted with 40% ethanol. The eluate was concentrated under reduced pressure and crude lemon flavonoids were obtained. Eriocitrin was prepared from crude flavonoids using preparative HPLC (LC-8A; Shimadzu, Kyoto, Japan) using a YMC-Pack ODS column (50 × 250 mm; YMC, Kyoto, Japan). The purity was determined as >96% using HPLC (LC-10A; Shimadzu).

Feeding zebrafish and experimental design. Adult zebrafish (AB line; Zebrafish International Resource Center, Eugene, OR, USA) were kept at 28°C under a 14 h light : 10 h dark cycle, and water conditions of environmental quality were maintained as previously described[52]. Zebrafish were assigned into each dietary group for 2 or 4 weeks with five fish per 1.7-L tank. From 3.5 mpf, zebrafish in the OF group were fed three times per day with *Artemia* (60 mg cysts/fish/day; Miyako Kagaku, Tokyo, Japan), and the control group were fed once daily in the morning (~09:00 h), as described previously[13]. Compared with flake foods that have also been used to feed zebrafish[52], the amounts of fat and protein in *Artemia* are higher and lower, respectively, whereas the amount of carbohydrate is comparable[53]. Zebrafish fed 5 or 60 mg/day freshly hatched *Artemia* consumed about 80% and 50% of the provided *Artemia*, respectively, translating to 20 and 150 cal. Maintenance energy requirement for zebrafish is <30 cal[54], therefore, it seemed reasonable to induce DIO-zebrafish by this overfeeding protocol. For the eriocitrin-feeding experiments, gluten granules (Wako Pure Chemical Industries, Tokyo, Japan) containing 0.8–1.4% eriocitrin were prepared as described previously[55]. Zebrafish were fed the eriocitrin-containing granules (2 mg/day) 20 min before *Artemia* feeding in the morning. We confirmed that 20 min was sufficient for eating these granules during the feeding experiment. After the experiments, the fish were sacrificed by an overdose of anaesthetic solution tricaine methanesulfonate (500 mg/L; Sigma–Aldrich, St. Louis, MO, USA) in distilled water.

Measurement of body weight, plasma TG and blood glucose. The body weight and length of zebrafish were measured weekly throughout the study as described previously[13,20]. For the blood chemistry analyses, zebrafish were deprived of food overnight and blood was withdrawn from the dorsal artery by a heparinized glass capillary needle (GD-1; Narishige, Tokyo, Japan) at the indicated times. Blood glucose[20] and plasma TG[13] were measured as described previously.

Oil Red O staining. Liver tissues were collected from zebrafish by surgical manipulation under a stereoscopic microscope (MZ16F; Leica Microsystems, Wetzlar, Germany). The livers were fixed in Histo-Fresh (Falma, Tokyo, Japan) and embedded in Tissue-Tek (Sakura Finetek, Tokyo, Japan) and dissected in a cryostat (Microm HM-550; Thermo Fisher Scientific, Waltham, MA, USA). The sections were stained with Oil Red O (Wako Pure Chemical Industries) as described previously[20]. Lipid droplets within the cells were stained with Oil Red O dye as described previously[56]. After image capture using an Axiovert 200 M microscope (Zeiss, Thornwood, NY, USA), intracellular lipid accumulation was quantified by measurement of OD_{520} using the Victor2 multilabel plate reader (PerkinElmer, Boston, MA, USA).

DNA microarray experiments. Liver tissues were collected from DIO-zebrafish for each experimental condition. Livers were fixed in RNAlater (Applied Biosystems, Foster City, CA, USA) at 4°C for 1 day. The liver tissues were immersed in 1 ml Isogen (NipponGene, Tokyo, Japan) and homogenized using the Mixer Mill MM 300 (Retsch, Haan, Germany) with 5-mm zirconia beads (BioMedicalScience, Tokyo, Japan) for 3 min at 25 Hz. After homogenization, total RNA was extracted according to the protocol for Isogen, in combination with the clean-up protocol of the RNeasy Mini Kit (Qiagen, Hilden, Germany). The DNA microarray experiments were conducted using the Low RNA Input Fluorescent Linear Amplification Kit (Agilent Technologies, Santa Clara, CA, USA) and G2518A Agilent Zebrafish Whole Genome Oligo Microarrays (Agilent Technologies), as previously described[20]. The hybridized microarrays were scanned (Agilent G2565BA microarray scanner) and quantified using Feature Extraction software (Agilent Technologies). One-way analysis of variance (ANOVA) was performed to identify differentially expressed probes ($P < 0.01$). k-means clustering was conducted using MultiExperiment Viewer MeV4, a module of TM4 microarray analysis software[57]. The probes were converted to human orthologues using the Life Science Knowledge Bank (World Fusion, Tokyo, Japan). GSEA and SNEA were conducted using Pathway Studio 7 (Ariadne Genomics, Rockville, MD, USA).

Cell culture and treatment. HepG2 human hepatocarcinoma cells were cultured in Dulbecco's modified Eagle's medium (DMEM; Invitrogen, Carlsbad, CA, USA), supplemented with 100 μg/ml streptomycin sulphate (Sigma–Aldrich), 100 U/ml penicillin G (Sigma–Aldrich) and 10% (v/v) foetal bovine serum (FBS; Invitrogen), and maintained at 37°C in an atmosphere of 5% CO_2 and 95% air. Sodium palmitate was dissolved in preheated 0.1 N NaOH and diluted in DMEM containing 1.76% (w/v) bovine serum albumin (BSA), to give a final palmitate concentration of 400 μM, as described previously[58]. Palmitate was administered after 48 h treatment with eriocitrin.

qRT-PCR of zebrafish and cultured cells. For liver tissues of adult zebrafish, total RNA of each sample was purified as described above. For young zebrafish, eight fish were homogenized in RLT buffer using the Mixer Mill 300. Total RNA was purified using the RNeasy Mini Kit (Qiagen), according to the manufacturer's protocol. For cultured cells, total RNA was also purified using the RNeasy Mini Kit. First-strand cDNA was prepared with 200 ng total RNA using the Super Script III First-strand System (Life Technologies, Gaithersburg, MD, USA) with random primers (Life Technologies). qRT-PCR was performed with Power SYBR Green Master Mix (Applied Biosystems) in triplicate, according to the manufacturer's protocol. The sequences of the primers are shown in Supplementary Table S3. The oligonucleotides of these primers were synthesized by Life Technologies.

qRT-PCR for measurement of mtDNA. DNA was extracted using phenol/chloroform precipitation and stored in water at −80°C until analysis[59]. Purity and concentration of DNA recovered were determined with a NanoDrop spectrophotometer. Real-time PCR was performed with Power SYBR Green PCR mix (Applied Biosystems) in an ABI 7300 Real Time PCR System (Applied Biosystems). Quantification of mtDNA was accomplished by calculating the ratio of a mitochondrion-encoded gene (*CYTB*) to a nuclear-encoded gene (*PK*), and expressing it as mtDNA copy number per cell.

Measurement of mitochondrial size. HepG2 cells were seeded at 5×10^4 cells/ml in tissue-culture-treated μ-slide eight-well plates (ibidi, Martinsried, Germany), and incubated for 48 h with or without eriocitrin. The cells were stained with MitoTracker Red CMXRos (Molecular Probes, Eugene, OR, USA) and Hoechst 33342 (Dojindo, Tokyo, Japan) for 15 min. The final concentration of each fluorescent dye was 1 μM for Mitotracker Red and 40 μg/ml for Hoechst 33342. Cells were rinsed with phosphate-buffered saline, and fresh medium was added. Cells were visualized using a fluorescent Zeiss Axiovert 200 M (Carl Zeiss MicroImaging, Thornwood, NY, USA) and analysed using ImageJ software (National Institutes of Health, Bethesda, MD, USA).

ATP quantification. For the zebrafish study, 4 dpf zebrafish were exposed to eriocitrin for 3 days in E3 medium (5 mM NaCl, 0.17 mM KCl, 0.4 mM $CaCl_2$ and 0.16 mM $MgSO_4$) at 28°C. Zebrafish were transferred to collection microtubes (Qiagen) with 100 μl E3 medium. One hundred microliters of CellTiter-Glo luminescent cell viability assay reagent (Promega, Madison, WI, USA) was added to each tube containing zebrafish. The zebrafish were homogenized quickly using the Mixer Mill 300.

For the cell-based study, HepG2 cells were seeded in 96-well microplates at 2.0×10^4 cells/well in 100 μl growth medium. Cells were incubated at 37°C for 3 days with eriocitrin. Before the ATP assay started, cell numbers in each well were measured using Calcein-AM (Dojindo), according to the manufacturer's instructions. After that, the ATP measurements (CellTiter-Glo luminescent cell viability assay) were performed according to the manufacturer's instructions. Fluorescence and luminescence were measured by Victor2 fluorescent plate reader (PerkinElmer).

Eriocitrin toxicity in zebrafish. Zebrafish embryos were exposed to eriocitrin from 6 hpf to 5 dpf. The number of survivors was counted under a MZ16F stereoscopic microscope (Leica Microsystems). One hour before evaluation of locomotor activity, a fish was removed from each experimental unit and placed in a well with 50 μl of E3 medium in a 96-well, clear-bottom plate for acclimatization. The fish were then video-recorded for 15 min. The resulting footage was evaluated to measure the swimming distance using the EthoVision XT system ver8.0 (Noldus Information Technology, Wageningen, The Netherlands) as described previously[60].

Statistical analysis. All data were represented as mean ± SEM. Differences between the two groups were examined for statistical significance using Student's *t* test. For multiple comparisons, we used one-way ANOVA followed by Bonferroni–Dunn multiple comparison. $P < 0.05$ was considered to denote statistical significance.

1. Pagano, G. *et al.* Nonalcoholic steatohepatitis, insulin resistance, and metabolic syndrome: further evidence for an etiologic association. *Hepatology* **35**, 367–372 (2002).
2. Moore, J. B. Non-alcoholic fatty liver disease: the hepatic consequence of obesity and the metabolic syndrome. *Proc Nutr Soc* **69**, 211–220 (2010).
3. Raszeja-Wyszomirska, J., Lawniczak, M., Marlicz, W., Miezynska-Kurtycz, J. & Milkiewicz, P. [Non-alcoholic fatty liver disease--new view]. *Pol Merkur Lekarski* **24**, 568–571 (2008).
4. Wree, A., Kahraman, A., Gerken, G. & Canbay, A. Obesity affects the liver - the link between adipocytes and hepatocytes. *Digestion* **83**, 124–133 (2011).
5. Jung, U. J., Lee, M. K., Jeong, K. S. & Choi, M. S. The hypoglycemic effects of hesperidin and naringin are partly mediated by hepatic glucose-regulating enzymes in C57BL/KsJ-db/db mice. *J Nutr* **134**, 2499–2503 (2004).
6. Bok, S. H. *et al.* Plasma and hepatic cholesterol and hepatic activities of 3-hydroxy-3-methyl-glutaryl-CoA reductase and acyl CoA: cholesterol transferase are lower in rats fed citrus peel extract or a mixture of citrus bioflavonoids. *J Nutr* **129**, 1182–1185 (1999).
7. Gonzalez-Molina, E., Dominguez-Perles, R., Moreno, D. A. & Garcia-Viguera, C. Natural bioactive compounds of Citrus limon for food and health. *J Pharm Biomed Anal* **51**, 327–345 (2010).
8. Chiba, H. *et al.* Hesperidin, a citrus flavonoid, inhibits bone loss and decreases serum and hepatic lipids in ovariectomized mice. *J Nutr* **133**, 1892–1897 (2003).
9. Miyake, Y., Yamamoto, K., Morimitsu, Y. & Osawa, T. Characterristics of antioxidative flavonoid glycosides in lemon fruit. *Food Sci. Technol. Int. Tokyo* **4**, 48–53 (1998).
10. Minato, K. *et al.* Lemon flavonoid, eriocitrin, suppresses exercise-induced oxidative damage in rat liver. *Life Sci* **72**, 1609–1616 (2003).
11. Miyake, Y., Yamamoto, K., Tsujihara, N. & Osawa, T. Protective effects of lemon flavonoids on oxidative stress in diabetic rats. *Lipids* **33**, 689–695 (1998).
12. Miyake, Y. *et al.* Lipid-lowering effect of eriocitrin, the main flavonoid in lemon fruits, in rats on a high-fat and high-cholesterol diet. *J food science* **71**, 633–637 (2006).
13. Oka, T. *et al.* Diet-induced obesity in zebrafish shares common pathophysiological pathways with mammalian obesity. *BMC physiology* **10**, 21 (2010).
14. Lieschke, G. J. & Currie, P. D. Animal models of human disease: zebrafish swim into view. *Nat Rev Genet* **8**, 353–367 (2007).
15. Tanaka, T. *et al.* Pharmacogenomics of cardiovascular pharmacology: pharmacogenomic network of cardiovascular disease models. *J Pharmacol Sci* **107**, 8–14 (2008).
16. Kinkel, M. D. & Prince, V. E. On the diabetic menu: zebrafish as a model for pancreas development and function. *Bioessays* **31**, 139–152 (2009).
17. Wang, Z. *et al.* Zebrafish beta-adrenergic receptor mRNA expression and control of pigmentation. *Gene* **446**, 18–27 (2009).
18. Schlegel, A. & Stainier, D. Y. Lessons from "lower" organisms: what worms, flies, and zebrafish can teach us about human energy metabolism. *PLoS Genet* **3**, e199 (2007).
19. Flynn, E. J., 3rd, Trent, C. M. & Rawls, J. F. Ontogeny and nutritional control of adipogenesis in zebrafish (Danio rerio). *J Lipid Res* **50**, 1641–1652 (2009).
20. Tainaka, T. *et al.* Transcriptome analysis of anti-fatty liver action by Campari tomato using a zebrafish diet-induced obesity model. *Nutr Metab (Lond)* **8**, 88 (2011).
21. Hasumura, T. *et al.* Green tea extract suppresses adiposity and affects the expression of lipid metabolism genes in diet-induced obese zebrafish. *Nutr Metab (Lond)* **9**, 73 (2012).
22. Beissbarth, T. & Speed, T. P. GOstat: find statistically overrepresented Gene Ontologies within a group of genes. *Bioinformatics* **20**, 1464–1465 (2004).
23. Subramanian, A. *et al.* Gene set enrichment analysis: a knowledge-based approach for interpreting genome-wide expression profiles. *Proc Natl Acad Sci U S A* **102**, 15545–15550 (2005).
24. Berthiaume, J. & Wallace, K. B. Perfluorooctanoate, perflourooctanesulfonate, and N-ethyl perfluorooctanesulfonamido ethanol; peroxisome proliferation and mitochondrial biogenesis. *Toxicol Lett* **129**, 23–32 (2002).
25. Palmeira, C. M., Rolo, A. P., Berthiaume, J., Bjork, J. A. & Wallace, K. B. Hyperglycemia decreases mitochondrial function: the regulatory role of mitochondrial biogenesis. *Toxicol Appl Pharmacol* **225**, 214–220 (2007).
26. Clapham, J. C. & Storlien, L. H. The fatty acid oxidation pathway as a therapeutic target for insulin resistance. *Expert Opin Ther Targets* **10**, 749–757 (2006).
27. Bournat, J. C. & Brown, C. W. Mitochondrial dysfunction in obesity. *Curr Opin Endocrinol Diabetes Obes* **17**, 446–452 (2010).
28. Zhang, D. *et al.* Mitochondrial dysfunction due to long-chain Acyl-CoA dehydrogenase deficiency causes hepatic steatosis and hepatic insulin resistance. *Proc Natl Acad Sci U S A* **104** (2007).
29. Ibdah, J. A. *et al.* Mice heterozygous for a defect in mitochondrial trifunctional protein develop hepatic steatosis and insulin resistance. *Gastroenterology* **128**, 1381–1390 (2005).
30. Miyake, Y., Yamamoto, K., Morimitsu, Y. & Osawa, T. Isolation of C-glucosylflavone from lemon peel and antioxidative activity of flavonoid compounds in lemon fruit. *J. Agric. Food Chem.* **45**, 4619–4623 (1997).
31. Alam, M. A. *et al.* Naringin improves diet-induced cardiovascular dysfunction and obesity in high carbohydrate, high fat diet-fed rats. *Nutrients* **5**, 637–650 (2013).
32. Fukuchi, Y. *et al.* Lemon Polyphenols Suppress Diet-induced Obesity by Up-Regulation of mRNA Levels of the Enzymes Involved in beta-Oxidation in Mouse White Adipose Tissue. *J Clin Biochem Nutr* **43**, 201–209 (2008).
33. Seo, Y. S. *et al.* PPAR agonists treatment is effective in a nonalcoholic fatty liver disease animal model by modulating fatty-acid metabolic enzymes. *J Gastroenterol Hepatol* **23**, 102–109 (2008).
34. Xu, Z. *et al.* Liver-specific inactivation of the Nrf1 gene in adult mouse leads to nonalcoholic steatohepatitis and hepatic neoplasia. *Proc Natl Acad Sci U S A* **102**, 4120–4125 (2005).
35. Scarpulla, R. C. Transcriptional activators and coactivators in the nuclear control of mitochondrial function in mammalian cells. *Gene* **286**, 81–89 (2002).
36. Wu, Z. *et al.* Mechanisms controlling mitochondrial biogenesis and respiration through the thermogenic coactivator PGC-1. *Cell* **98**, 115–124 (1999).
37. Hempenstall, S., Page, M. M., Wallen, K. R. & Selman, C. Dietary restriction increases skeletal muscle mitochondrial respiration but not mitochondrial content in C57BL/6 mice. *Mech Ageing Dev* **133**, 37–45 (2012).
38. Rantanen, A., Jansson, M., Oldfors, A. & Larsson, N. G. Downregulation of Tfam and mtDNA copy number during mammalian spermatogenesis. *Mamm Genome* **12**, 787–792 (2001).
39. Kojima, H. *et al.* Mitochondrial abnormality and oxidative stress in nonalcoholic steatohepatitis. *Alcohol Clin Exp Res* **31**, S61–66 (2007).
40. Trauner, M., Arrese, M. & Wagner, M. Fatty liver and lipotoxicity. *Biochimica et biophysica acta* **1801**, 299–310 (2010).
41. Kotelnikova, E., Yuryev, A., Mazo, I. & Daraselia, N. Computational approaches for drug repositioning and combination therapy design. *J Bioinform Comput Biol* **8**, 593–606 (2010).
42. Duval, C., Fruchart, J. C. & Staels, B. PPAR alpha, fibrates, lipid metabolism and inflammation. *Arch Mal Coeur Vaiss* **97**, 665–672 (2004).
43. Francis, G. A., Fayard, E., Picard, F. & Auwerx, J. Nuclear receptors and the control of metabolism. *Annu Rev Physiol* **65**, 261–311 (2003).
44. Yotsumoto, T., Naitoh, T., Kanaki, T. & Tsuruzoe, N. A retinoid X receptor antagonist, HX531, improves leptin resistance without increasing plasma leptin level in KK-Ay mice under normal dietary conditions. *Metabolism* **54**, 573–578 (2005).
45. Nakatsuka, A. *et al.* RXR antagonism induces G0/G1 cell cycle arrest and ameliorates obesity by up-regulating the p53-p21(Cip1) pathway in adipocytes. *J Pathol* **226**, 784–795 (2012).
46. Satih, S. *et al.* Expression analyses of nuclear receptor genes in breast cancer cell lines exposed to soy phytoestrogens after BRCA2 knockdown by TaqMan Low-Density Array (TLDA). *J Mol Signal* **4**, 3 (2009).
47. Crespillo, A. *et al.* Reduction of body weight, liver steatosis and expression of stearoyl-CoA desaturase 1 by the isoflavone daidzein in diet-induced obesity. *Br. J. Pharmacol* **164**, 1899–1915 (2011).
48. Yoshikawa, T. *et al.* Identification of liver X receptor-retinoid X receptor as an activator of the sterol regulatory element-binding protein 1c gene promoter. *Mol Cell Biol* **21**, 2991–3000 (2001).
49. Wang, G. L. *et al.* Resveratrol inhibits the expression of SREBP1 in cell model of steatosis via Sirt1-FOXO1 signaling pathway. *Biochem Biophys Res Commun* **380**, 644–649 (2009).
50. Pessayre, D., Mansouri, A. & Fromenty, B. Nonalcoholic steatosis and steatohepatitis. V. Mitochondrial dysfunction in steatohepatitis. *Am J Physiol Gastrointest Liver Physiol* **282**, G193–199 (2002).
51. Miyake, Y., Yamamoto, K. & Osawa, T. Metabolism of Antioxidant in Lemon Fruit (Citrus limon BURM. f.) by Human Intestinal Bacteria. *J. Agric. Food Chem.* **45**, 3738–3742 (1997).
52. Monte, W. The Zebrafish Book: A guide for the laboratory use of zebrafish. (*Danio rerio*) 4th edition. (Univ. of Oregon Press, Eugene, 2000).

53. Bengtson, D. L. P. & Sorgeloos, P. Use of Artemia as Food Source. *Artemia Biology*, 255–286 (1991).
54. Pannevis, M. C. & Earle, K. E. Maintenance energy requirement of five popular species of ornamental fish. *J Nutr* **124**, 2616S–2618S (1994).
55. Zang, L., Morikane, D., Shimada, Y., Tanaka, T. & Nishimura, N. A novel protocol for the oral administration of test chemicals to adult zebrafish. *Zebrafish* **8**, 203–210 (2011).
56. Ramirez-Zacarias, J. L., Castro-Munozledo, F. & Kuri-Harcuch, W. Quantitation of adipose conversion and triglycerides by staining intracytoplasmic lipids with Oil red O. *Histochemistry* **97**, 493–497 (1992).
57. Saeed, A. I. *et al*. TM4: a free, open-source system for microarray data management and analysis. *Biotechniques* **34**, 374–378 (2003).
58. Liu, J. F. *et al*. Reduction of lipid accumulation in HepG2 cells by luteolin is associated with activation of AMPK and mitigation of oxidative stress. *Phytother Res* **25**, 588–596 (2011).
59. Strauss, W. M. Preparation of genomic DNA from mammalian tissue. *Curr Protoc Mol Biol* **Chapter 2**, Unit2 (2001).
60. Shimada, Y., Hirano, M., Nishimura, Y. & Tanaka, T. A high-throughput fluorescence-based assay system for appetite-regulating gene and drug screening. *PLoS One* **7**, e52549 (2012).

Acknowledgments

This work was supported in part by KAKENHI (24590318), the New Energy and Industrial Technology Development Organization, and the Japan Chemical Industry Association. We would like to thank K. Nishiguchi and M. Ariyoshi for their experimental assistance and R. Ikeyama for secretarial assistance.

Author contributions

M.H. and Y.S. conducted animal and cell-based experiments and prepared the manuscript. J.K. prepared the zebrafish. J.K. and Z.L. also conducted animal experiments. T.I. and T.K. purified eriocitrin and evaluated its purity. Y.N. conducted statistical analyses. T.K., N.N. and T.T. planned the experiments. T.T. modified the manuscript.

Additional information

Supplementary information accompanies this paper at http://www.nature.com/scientificreports

Competing financial interests: The authors declare no competing financial interests.

How to cite this article: Hiramitsu, M. *et al*. Eriocitrin ameliorates diet-induced hepatic steatosis with activation of mitochondrial biogenesis. *Sci. Rep.* **4**, 3708; DOI:10.1038/srep03708 (2014).